

This is an Open Access document downloaded from ORCA, Cardiff University's institutional repository: <https://orca.cardiff.ac.uk/id/eprint/151992/>

This is the author's version of a work that was submitted to / accepted for publication.

Citation for final published version:

Lu, Yongtao, Yang, Zhuoyue, Zhu, Hanxing and Wu, Chengwei 2023. Predicting the effective compressive modulus of human cancellous bone using the conventional neural network method. *Computer Methods in Biomechanics and Biomedical Engineering* 26 (10) , pp. 1150-1159. 10.1080/10255842.2022.2112183

Publishers page: <https://doi.org/10.1080/10255842.2022.2112183>

Please note:

Changes made as a result of publishing processes such as copy-editing, formatting and page numbers may not be reflected in this version. For the definitive version of this publication, please refer to the published source. You are advised to consult the publisher's version if you wish to cite this paper.

This version is being made available in accordance with publisher policies. See <http://orca.cf.ac.uk/policies.html> for usage policies. Copyright and moral rights for publications made available in ORCA are retained by the copyright holders.



1 **Predicting the effective elastic property of human cancellous**
2 **bone using the convolutional neural network method**

3
4 Yongtao Lu^{1,2,3*}, Zhuoyue Yang¹, Hanxing Zhu⁴, Chengwei Wu^{1,2*}
5

6 ¹Department of Engineering Mechanics, Dalian University of Technology,

7 ²State Key Laboratory of Structural Analysis for Industrial Equipment, Dalian
8 University of Technology, No. 2 Linggong Road, 116024, Dalian, China

9 ³DUT-BSU Joint Institute, Dalian University of Technology, Dalian, 116024, China

10 ⁴School of Engineering, Cardiff University, Cardiff, UK
11

12 Corresponding author:

13 Prof. Chengwei Wu

14 Department of Engineering Mechanics,

15 Dalian University of Technology

16 No.2 Linggong Road, 116024, Dalian, China

17 Email: cwwu@dlut.edu.cn
18
19

20 Number of words (Introduction to conclusion): 3626

21 Number of figures: 9

22 Number of tables: 0
23

1 **Abstract**

2
3 The efficient prediction of biomechanical properties of bone plays an important role
4 in the assessment of bone quality. However, the present techniques are either of low
5 accuracy or of high complexity for the clinical application. The present study aims to
6 investigate the predictive ability of the evolving convolutional neural network (CNN)
7 technique in predicting the effective compressive modulus of porous bone structures.
8 The T11/T12/L1 segments of thirty-five female cadavers were scanned using the
9 HR-pQCT scanner and the images obtained from it were used to generate 10896 2 D
10 bone samples, in which only the cancellous bony parts were processed and
11 investigated. The corresponding 10896 heterogeneous finite-element (FE) models
12 were generated, and then a CNN model was constructed and trained using the
13 predictions of the FE analysis as the ground truths. Then the remaining 260 bone
14 samples generated from the initial HR-pQCT images were used to test the predictive
15 power of the CNN model. The results show that the coefficient of the determinant (R^2)
16 from the linear correlation between the CNN and FE predicted elastic modulus is 0.95,
17 which is much higher than that from the correlation between the BMD and the FE
18 predictions ($R^2 = 0.65$). Furthermore, the 95th and 50th percentiles of relative
19 prediction error are below 0.28 and 0.09, respectively. In the conclusion, the CNN
20 model can efficiently predict the effective compressive modulus of human cancellous
21 bone and can be used as a promising and clinically applicable method to evaluate the
22 mechanical quality of porous bone.

23
24 **Keywords:** Convolutional neural network, cancellous bone, mechanical property,
25 prediction error

1 **1. Introduction**

2 Prediction of the mechanical properties of the human bone tissues is of great
3 importance for the assessment, prevention and early treatment of bone fracture.
4 Currently, using the measurements of the bone mineral density (BMD), such as the
5 areal bone mineral density (aBMD) obtained from the dual energy X-ray
6 absorptiometry (DXA) and the volumetric BMD (vBMD) obtained from the
7 quantitative computed tomography (QCT), are widely used in clinic. However, the
8 aBMD obtained from the DXA contains neither the information on the bone
9 microarchitecture nor any mechanical property of the bone tissues, and the vBMD
10 cannot provide information on the distribution of the BMD and the bone
11 microarchitecture. Because the increasing risk of bone fracture is caused not only by
12 the loss of bone mass but also by the deterioration of the bone microarchitecture,
13 neither aBMD nor vBMD can provide a good prediction of the mechanical property
14 of the bone tissues and approximately only 50% of the variability in the vertebral
15 fracture can be predicted by these BMD measurements (**Dong et al., 2018; Ebbesen**
16 **et al., 2000; Lochmueller et al., 2002; Lu et al., 2015**).

17 In the last a couple of decades, the subject-specific finite element (FE) models of
18 bone tissues have been widely used to predict the mechanical properties of bone
19 tissues (**Chevalier et al., 2009; Lu et al., 2014, 2019; Pistoia et al., 2002; Wang et**
20 **al., 2012**). It has been demonstrated that the three-dimensional (3D) FE models of
21 bone have a higher ability for predicting the bone fracture loads than the densitometry
22 measurements (aBMD and vBMD) (**Lu et al., 2014; Wang et al., 2012**). However,
23 because of the high complexity in generating the 3D FE models of bone tissues
24 (including the process of segmenting the bone tissues, mesh generation, etc.) and the
25 high cost in performing the FE calculations, it is very challenging to transfer the
26 subject-specific 3D FE modeling into the clinic for the routine use. In the recent years,
27 the machine learning technique, e.g., the convolutional neural network (CNN), has
28 emerged as a novel and crucial tool for predicting the properties of porous structures
29 (**Alber et al., 2019; Alastruely-Lopez et al., 2020; Chandran et al., 2018; Rane et**
30 **al., 2019**). For examples, Chandran et al. have managed the accurate prediction of the

1 thickness of cortex using the supervised machine learning algorithm (**Chandran et al.,**
2 **2018**); Rane et al. have managed the accurate prediction of the force of the skeletal
3 muscles using the deep learning algorithm (**Rane et al., 2019**); Alastruely-Lopez et al.
4 have developed the artificial neural network model to predict the impingement and the
5 dislocation in the total hip arthroplasty (**Alstruey-Lopez et al., 2020**). In principal,
6 the CNN technique takes the medical images, the patient's information (such as the
7 gender, age), etc. as the input and then establishes the relationship between the input
8 variables and the output (such as the bone fracture risk, etc.) using the learning
9 process based on a large amount of datasets. Therefore, compared to the
10 subject-specific FE modeling technique, the CNN technique has the clear advantages
11 of being efficient, accurate and real-time and has the potential for the direct clinic
12 routine use. Despite these, to the best of our knowledge, the application of the CNN
13 technique in predicting the mechanical property of the vertebral bone tissues using the
14 CT data has not been fully elaborated.

15 The aim of the present study was to assess the capability of the CNN method in
16 predicting the mechanical property of the human cancellous bone tissues based on a
17 large amount of the CT images of bone tissues.

19 **2. Materials and Method**

20 **2.1. CT image datasets of the human cancellous bone**

21 The high resolution CT images (HR-pQCT) of human cancellous bone instead of
22 the clinical CT images were used in the present study, because the bone samples were
23 from the elderly female patients and the microarchitecture of these bone tissues can be
24 hardly characterized in the regular clinical CT images. The detailed procedure for the
25 acquisition of the HR-pQCT images of the vertebral specimens is described in the
26 previous studies (**Lu et al., 2014; 2015**). In brief, thirty-five cadavers were harvested
27 from female patients with a mean age of 81.3 ± 7.2 year-old (range: 65 to 90
28 year-old). The spinal segment of T11/T12/L1 was dissected and the specimens were
29 scanned during frozen using the HR-pQCT scanner (XtremeCT, Scanco Medical AG,

1 Bruettisellen, Switzerland) operating at 59.4 kV, 900 μ As with an image voxel size of
2 $82.0 \times 82.0 \times 82.0 \mu\text{m}^3$.

3 4 **2.2. The effective elastic modulus of the bone from the finite element analysis**

5 The effective elastic moduli of the cancellous bone tissues calculated from the FE
6 models were taken as the ground truth and used to train the CNN model constructed
7 in the present study. To obtain the effective elastic modulus, the heterogeneous FE
8 model of the human cancellous bone was created using the method previously
9 developed (Lu et al., 2019). In brief, first, a volume of interest was cropped out from
10 the vertebral body, which contained only the cancellous bone part (Figure 1). Second,
11 the grayscale image datasets were smoothed using a Gaussian filter (sigma = 1.2,
12 support = 2.0) to reduce the influence of the image noise and then each image voxel
13 was converted to a two-dimensional (2D) 4-node plane stress element (PLANE182).
14 In the FE mesh model generated, the heterogenous material model was defined by
15 converting the image grayscale values to the corresponding Young's moduli (Figure
16 2). The image grayscale values were first converted into the vBMD values based on
17 the linear calibration equation provided by the HR-pQCT scanner. The vBMD values
18 were then converted into the bone ash densities using the relationship reported in the
19 literature, i.e., $\rho_{ash} = 0.877 \times \rho_{HA} + 0.079$ (ρ_{ash} is the bone ash density, unit in
20 mg/cm^3 ; ρ_{HA} is the HA-equivalent vBMD, unit in mg/cm^3) (Knowles et al., 2016).
21 Young's modulus of each bone element was then calculated from the bone ash density
22 using the following exponential density-modulus relationship (Knowles et al., 2016):

$$23 \quad E = \begin{cases} 0.1127 \times 1200^{1.746}, & \rho_{ash} > 1200 \\ 0.1127 \times \rho_{ash}^{1.746}, & 400 \leq \rho_{ash} \leq 1200 \\ 0.0104, & \rho_{ash} < 400 \end{cases} \quad (1)$$

24 In the above definition, an upper threshold of $1200.00 \text{ mg}/\text{cm}^3$ was set to eliminate the
25 effect of the artificially high grayscale values. On the other hand, the material with the
26 bone ash density lower than $400 \text{ mg}/\text{cm}^3$ was regarded as the bone marrow, and the
27 corresponding Poisson's ratio was set to 0.49 (Crawford et al., 2003). The Poisson's
28 ratio for the bone elements was set to 0.30. An example of the heterogeneous FE

1 model is shown in **Figure 2(b)**, where the color map shows the distribution of the
 2 tissue Young's modulus and the black areas represent the pores.

3 The representative volume element (RVE) method was used to calculate the
 4 effective elastic properties of the cancellous bone, which has been widely used to
 5 calculate the mechanical properties of complex composites (**Omairey et al., 2019**). In
 6 the present study, the FE model of the 2D bone sample was taken as the RVE and
 7 periodic boundary conditions (PBCs) were applied to the RVE, which can be
 8 expressed as:

$$9 \quad u_i^{b+} - u_i^{b-} = \bar{\varepsilon}_{ik} \Delta x_k^b \quad (2)$$

10 where, u_i^{b+} and u_i^{b-} are the displacements on a pair of nodes x_k^{b+} and x_k^{b-} of
 11 two opposite boundary surfaces, and $\Delta x_k^b = x_k^{b+} - x_k^{b-}$ with the superscript b
 12 indicating a quantity pertaining to boundary.

13 The elastic stiffness components C_{ijkl} can be determined from the calculation
 14 results of RVE by:

$$15 \quad \bar{\sigma}_{ij} = C_{ijkl} \bar{\varepsilon}_{kl} \quad (3)$$

16 In the present study, a plane stress problem is assumed and thus the effective
 17 Young's modulus E of the cancellous bone can be derived as:

$$18 \quad E = \frac{C_{1111} + C_{2222}}{2} (1 - \nu^2) \quad (4)$$

19 where, ν is the Poisson's ratio and

$$20 \quad \nu = \frac{2C_{1122}}{C_{1111} + C_{2222}} \quad (5)$$

21 To enable the process of a large amount of the bone samples, all the
 22 pre-processing and post-processing were automated using the in-house developed
 23 Matlab (R2019, MathWorks, Natick, Massachusetts, U.S.A.) code and the finite
 24 element analysis was performed using the Ansys APDL (v18.0, ANSYS, Inc.,
 25 Canonsburg, PA, U.S.A.).

27 **2.3. Training and cross-validation of the CNN model**

28 In the present study, a convolutional neural network (CNN) model was developed
 29 to predict the effective elastic modulus of the vertebral cancellous bone. The

1 procedure for the training and testing of the CNN model is presented in **Figure 3**. The
2 training process of the CNN model can be briefly described as below: 10636 2D
3 human vertebral cancellous bone samples covering a large range of the bone
4 porosities and bone microarchitectures were processed. Their effective Young's
5 moduli were calculated from the FE analysis and served as the ground truth for the
6 effective modulus of the cancellous bone tissue. The distribution of the effective
7 elastic moduli of the bone samples is shown in **Figure 4**, where the 50th percentile of
8 the elastic moduli is 988.7 MPa. The 10636 bone samples were randomly divided into
9 two parts: one part has 8000 samples used for training the CNN model and the other
10 has 2636 samples used for the cross-validation of the CNN model.

11 The CNN model constructed is shown in **Figure 5**, which can be briefly
12 described as below: First, several nonlinear layers were applied to gradually extract
13 the features in the bone images; afterwards, the grayscale CT image was transformed
14 to a numerical value as the output of the CNN. In the present study, the grayscale
15 image with the size of $14.9 \times 14.9 \text{ mm}^2$ (182×182) was taken as the input for the
16 CNN model. Eight convolution layers, four pooling layers and four fully connected
17 layers were applied to the image. The convolution kernels were trained in a
18 hierarchical manner, which consisted of the low-level features to generate more
19 complex patterns. The size of all the convolution kernels was set to 3×3 . The
20 maximal pooling was applied after the convolutional layers to simplify the
21 information of the output neurons (**Li et al., 2019**). To improve the accuracy of the
22 CNN model, the 20% dropout was used in the four pooling layers, and the batch
23 normalization was used to mitigate the effects of the initialization and to accelerate
24 the training of the CNN model (**Li et al., 2019**). In the present study, the grayscale
25 images of the human vertebral cancellous bone tissues were taken as the input for the
26 CNN model constructed and the corresponding effective elastic modulus for each
27 bone sample was the output from the CNN model.

28 In the training process, the CNN model learned the valid representation
29 describing the geometric features of the vertebral cancellous bone tissues and
30 discarded those features less important. A loss function was defined to quantify the

1 difference between the effective elastic moduli predicted from the CNN model and
2 those calculated from the FE analysis. Then, the kernels and biases in the
3 convolutional layers and the weights in the fully connected layers were adjusted using
4 the backpropagation algorithm (**Rubio et al., 2011**). Iterative adjustments were made
5 to minimize the loss function using a large amount of bone image datasets. In the
6 present study, the mean absolute error (MAE) was set as the objective function:

$$7 \quad \text{MAE}[Y, f(X)] = \frac{1}{n} \sum_{i=1}^n |Y - f(X)| \quad (6)$$

8 where, Y is the effective elastic modulus of the bone tissues calculated from the FE
9 analysis; $f(X)$ is the corresponding effective elastic modulus calculated from the
10 CNN model and n is the number of samples used for the cross-validation ($n = 2636$
11 in the present study).

12 The training process was conducted on a desktop computer with the setting of
13 i7-8700 CPU, 32G RAM, and the Nvidia GTX1060. The batch size was set to 128
14 and the training was iterated for 200 epochs. The training process took approximately
15 2.0 hours.

16 **2.4. Predictive power of the CNN model**

17 To assess the predictive power of the CNN model constructed, 260 new bone
18 samples were processed. The effective elastic moduli of these bone samples were
19 calculated using the trained CNN model and the FE analysis, respectively. The FE
20 predictions were served as the ground truth and the predictive power of the CNN
21 model was obtained by comparing the values obtained from the CNN and the FE
22 models (**Figure 3b**). To quantify the accuracy of the CNN model, the relative
23 prediction error (RPE) was used, which is defined as below:

$$24 \quad \text{RPE} = \frac{|P^{\text{CNN}} - P^{\text{RVE}}|}{P^{\text{RVE}}} \times 100\% \quad (7)$$

25 where, P^{CNN} is the effective elastic modulus calculated from the CNN model, P^{RVE} is
26 the corresponding value calculated from the FE analysis.

28 **3. Results**

29 **3.1 Training and cross-validation of the CNN model**

1 The relation between the mean absolute error (MAE) and the training iteration is
2 shown in **Figure 6**. Because the initial values of the weights and biases are randomly
3 assigned, the MAE at the first a few iterations is high. However, after several
4 iterations, the MAE rapidly descends and the MSE is below 100.0 MPa after 100
5 training epochs. Therefore, no over-fitting is observed in the cross-validation.

6 **3.2 Predictive power of the CNN model**

7 The comparison using the 260 testing bone samples shows that the predictions
8 from the CNN model are highly correlated with those from the FE analysis ($R^2 =$
9 0.91). The slope of the correlation line is 0.79, which is a bit deviated away from the
10 diagonal line ($y = x$) (**Figure 7**), implying that some prediction errors are present in
11 the CNN model. The distribution of the relative prediction error (RPE) shows that
12 95th and 50th percentiles of the relative prediction error are below 0.28 and 0.09,
13 respectively (**Figures 8 and 9**).

15 **4. Discussion**

16 In the present study, a convolutional neural network (CNN) model for the quick
17 and accurate prediction of the elastic mechanical property of the porous bone tissues
18 was presented. The predictive power of the CNN model was assessed, and a good
19 accuracy was achieved, i.e., the 95th and 50th percentiles of the relative prediction
20 error are below 0.28 and 0.09, respectively.

21 The present study was motivated by the lengthy and complex nature of the
22 nonlinear FE analysis on human bone tissues. To obtain the effective mechanical
23 property of human bone, in the previous studies (**Lu et al. 2014; 2019**), it took more
24 than 8 hours to obtain the result using the 3D FE modeling technique (including the
25 image processing, the FE model generation, the nonlinear calculation, etc.), and more
26 than 4 hours to obtain the result using the 2D FE modeling technique. In contrast, it
27 takes only less than one minute to obtain the result using the CNN technique without
28 compromising the predictive power. The quick and accurate prediction of the effective
29 mechanical property of bone tissues is crucial in the clinical settings, because in the
30 scenario of bone trauma, a surgical plan has to be quickly decided, which can only be

1 made possible by a quick and accurate assessment of the bone quality. Additionally,
2 the ‘easy to use’ feature of the CNN technique is another important factor in the
3 clinical setting because the tool has to be easily operable by the clinical staff. The
4 CNN technique takes only the 2D CT images of the bone tissues as the input and can
5 quickly output the effective mechanical properties of the bone tissues within a few
6 minutes and thus meets the requirements. In the present study, to obtain the effective
7 elastic modulus of the bone tissue, it takes approximately 40 minutes using the FE
8 analysis (including the process of the image segmentation, the model generation, the
9 FE calculation, the post-processing, etc.), but it only takes approximately 30 seconds
10 using the CNN model constructed.

11 In the present study, the machine learning (ML) method of the CNN was used.
12 Compared to other ML techniques, e.g., the support vector machine (**Hao, 2009**), the
13 CNN is the most appropriate one for the specific challenges presented in the present
14 study. First, the CNN model takes the medical image, which is readily available in the
15 clinic, as the input. Second, the CNN technique uses the convolution kernel to extract
16 the features from the medical image and consequently the model parameters and
17 complexity are largely reduced (**Li et al., 2019; Ye et al., 2019**).

18 In the present study, the 95th and 50th percentiles of the relative prediction error
19 are below 0.28 and 0.09, respectively, which are comparable to the values reported in
20 the literature for solving the similar problems. For examples, Ye et al. developed the
21 deep neural network method for predicting the mechanical properties of porous
22 composites and a relative error of smaller than 3.0% was achieved (**Ye et al., 2019**);
23 Li et al. developed the deep learning method for predicting the effective mechanical
24 property of heterogeneous materials and a relative error below 3.0% was reported (**Li**
25 **et al., 2019**); Jiang et al. developed the support vector machine model for predicting
26 the hip fracture risk and an accuracy of 74.0% Area Under Curve (AUC) was
27 achieved. However, it should be noted that in the previous studies (**Jiang et al., 2015;**
28 **Li et al., 2019; Ye et al., 2019**), the large datasets are artificially generated using the
29 computer program, while the real clinical CT datasets are used in the present study.
30 Therefore, the factors, such as the image noise and the partial volume effect, are taken

1 into account in the CNN model constructed and consequently the results from the
2 present study can be of the direct clinical translation.

3 The present study showed that if a large amount of the clinical image datasets can
4 be obtained, the CNN model can be trained and used to predict the mechanical
5 property of the bone tissues. This is crucial for clinical applications. For example, the
6 model can be used to assess the bone fracture risk in case of a fall event
7 (**Bhattacharya et al., 2018**), to predict the long-term quality of the bone tissues so as
8 to help the design of the bone implant (**Metz et al., 2019**), etc. It should be noted that
9 not only one apparent mechanical property of the bone tissue (demonstrated in the
10 present study) can be predicted by the CNN technique, but also the distribution of the
11 stress/strain within the human tissue can be predicted using the CNN technique
12 (**Liang et al., 2018; Li et al., 2021**). Therefore, the CNN technique has the potential
13 to act as a surrogate for the FE method in the medical engineering analysis. Taking
14 use of the advanced ability of the CNN technique, i.e., the prediction of the strain
15 distribution in the bone region, the mechanically weakest region in the bone tissue can
16 be identified and consequently the specific bone region can be targeted for the
17 effective prevention and treatment of the bone fracture. It should be noted that in the
18 present study, the 2D numerical models are presented, which cannot consider the 3D
19 architecture of the cancellous bone tissues. Therefore, to achieve a higher power for
20 predicting the bone fracture risk, the future work should address the challenges related
21 the 3D problems, e.g., the collection of a large amount of the medical image datasets,
22 the automation of the processing of the 3D medical images, the automation of the 3D
23 FE analysis, etc.

24 Despite the advantages and potentials of the CNN technique, some limitations in
25 the present study should be discussed. First, the HR-pQCT images, which have a
26 higher image resolution than the regular clinical CT images, are used in the present
27 study. In the present study, the bone samples from the elderly donors are harvested
28 and their cancellous bone tissues have some extent of osteoporosis. Therefore, the
29 HR-pQCT images have to be used to accurately obtain the mechanical property of the
30 porous bone tissues. Although this complies with the aim of the present study, i.e., the

1 demonstration of the CNN technique in predicting the mechanical property of the
2 porous bone tissues, the feasibility study using the clinical CT images should still be
3 investigated in the future. Second, only the CT images of the bone tissue are taken as
4 the input for training the CNN model. The mechanical properties of the bone tissue
5 are determined not only by the tissue modulus and the microarchitecture of the bone
6 sample, but also by the factors such as the chemical compositions and gene sequence
7 which are not reflected in the medical CT images. Therefore, more input information,
8 such as the patient's body weight, gender, family medical history, etc., should also be
9 used for training the CNN model. The authors of the present study are in the process
10 of collecting a large amount of clinical datasets and investigating whether the
11 predictive power of the CNN model can be improved by adding more bone
12 information into the model training. Third, in the present study, the results from the
13 FE analysis are taken as the ground truth for the mechanical property of the bone
14 tissue. It should be noted that generally the results from the in vitro mechanical testing
15 should be taken as the ground truth (**Dong et al., 2018; Lu et al., 2014**), because
16 some behaviors of the bone tissue, such as the propagation of the bone micro crack,
17 can be hardly captured in the FE analysis. However, the mechanical property of the
18 bone tissue cannot be obtained from the in vitro testing in the clinical setting.
19 Furthermore, it has been shown in the previous studies (**Lu et al. 2014; 2019**) that the
20 predictions from the FE analysis have a high correlation with the results obtained
21 from the in vitro mechanical testing. Additionally, the aim of the present study is to
22 find an accurate and efficient surrogate approach for the FE analysis. Therefore, it is
23 reasonable to take the predictions from the FE analysis as the ground truth for
24 assessing the predictive power of the CNN model.

25 In conclusion, the convolutional neural network (CNN) technique can be used to
26 accurately and efficiently predict the mechanical properties of the porous cancellous
27 bone tissues. Compared to the FE modeling technique, the CNN technique can be
28 easily translated to the clinic for the routine use, e.g., the quick assessment of the bone
29 quality. It should be noted that the CNN technique can also be used to calculate other
30 physical properties of the porous/composite materials, e.g., the heat conductivity, the

1 fatigue life, the roughness (fracture toughness?), etc.

3 **Conflict of interest**

4 The authors declare that they do not have any financial or personal relationships
5 with other people or organizations that could have inappropriately influenced this
6 study.

8 **Acknowledgements**

9 This work was supported by the National Natural Science Foundation of China
10 (12072066, U1908233), the National Key R&D Program of China (2018YFA0704103,
11 2018YFA0704104) and the Liaoning Provincial Natural Science Foundation of China
12 (2019-MS-040).

15 **References**

- 16 Alastruey-Lopez, D., Ezquerro, L., Seral, B., Perez, M.A., 2020. Using artificial
17 neural networks to predict impingement and dislocation in total hip arthroplasty.
18 *Comput. Method. Biomech.* 23(4), 1-9.
- 19 Alber, M., Tepole, A.B., Cannon, W.R., De, S., Dura-Bernal, S., Garlkipati, K.,
20 Karniadakis, G.E., Lytton, W., Perdikaris, P., Petzold, L., Kuhl, E., 2019.
21 Integrating machine learning and multiscale modelling – perspective, challenges,
22 and opportunities in the biological, biomedical and behavioral sciences, *npj.*
23 *Digit. Med.* 115, 43-49.
- 24 Bhattacharya, P., Altai, Z., Qasim, M., Viceconti, M., 2018. A multiscale model to
25 predict current absolute risk of femoral fracture in a postmenopausal population.
26 *Biomech. Model. Mechan.* 18, 301-318.
- 27 Chandran, V., Maquer, G., Gerig, T., Zysset, P., Reyer, M., 2018. Supervised learning
28 for bone shape and cortical thickness estimation from CT images for finite
29 element analysis. *Med. Image. Anal.* 52, 42-55.
- 30 Chevalier, Y., Quek, E., Borah, B., Gross, G., Stewart, J., Lang, T., Zysset, P., 2009.
31 Biomechanical effects of teriparatide in women with osteoporosis treated

- 1 previously with alendronate and risedronate: results from quantitative computed
2 tomography-based finite element analysis of the vertebral body. *Bone*. 46(1),
3 41-48.
- 4 Crawford, R.P., Cann, C.E., Keaveny, T.M., 2003. Finite element models predict in
5 vitro vertebral body compressive strength better than quantitative computed
6 tomography. *Bone*. 33, 744-750.
- 7 Dong, X.N., Lu, Y., Matthias, K., Huber, G., Yan, C., Leng, H., Maquer, G., 2018.
8 Variogram-based evaluations of DXA correlate with vertebral strength, but do
9 not enhance the prediction compared to aBMD alone. *J. Biomech*. 77, 223-227.
- 10 Ebbesen, E.N., Thomsen, J.S., Beck-Nielsen, H., Nepper-Rasmussen, H.J., Mosekilde,
11 L., 2000. Lumbar vertebral body compressive strength evaluated by dual-energy
12 X-ray absorptiometry, quantitative computed tomography, and ashing. *Bone*.
13 25(6), 716-724.
- 14 Hao, P.Y., 2009. Interval regression analysis using support vector networks. *Fuzzy Set
15 Syst*, 160(17), 2466-2485.
- 16 Jiang, P., Missoum, S., Chen, Z., 2015. Fusion of clinical and stochastic finite element
17 data for hip fracture risk prediction. *Fuzzy Set Syst*. 48(15), 4043-4052.
- 18 Knowles, N.K., Reeves, J., Ferreira, L.M., 2016. Quantitative computed tomography
19 (QCT) derived bone mineral density in finite element studies: a review of the
20 literature. *J. Exp. Orthop*. 3(1), 36.
- 21 Li, G., Wang, H., Zhang, M., Tupin, S., Qiao, A., Liu, Y., Ohta, M., Anzai, H., 2021.
22 Prediction of 3D cardiovascular hemodynamics before and after coronary artery
23 bypass surgery via deep learning. *Commun. Biol*. 2021 ,4(1):99.
- 24 Li, X., Liu, Z., Cui, S., Luo, C., Li, C., Zhuang, Z., 2019. Predicting the effective
25 mechanical property of heterogeneous materials by image based modeling and
26 deep learning. *Comput. Method. Appl. M*. 347, 735-753.
- 27 Liang, L., Liu, M., Martin, C., Sun, W., 2018 A deep learning approach to estimate
28 stress distribution: a fast and accurate surrogate of finite element analysis. *J. R.
29 Soc. Interface*. 15, 20170844.
- 30 Lochmueller, E.M., Burklein, D., Kuhn, V., Glaser, C., Muller, R., Gluer, C.C.,

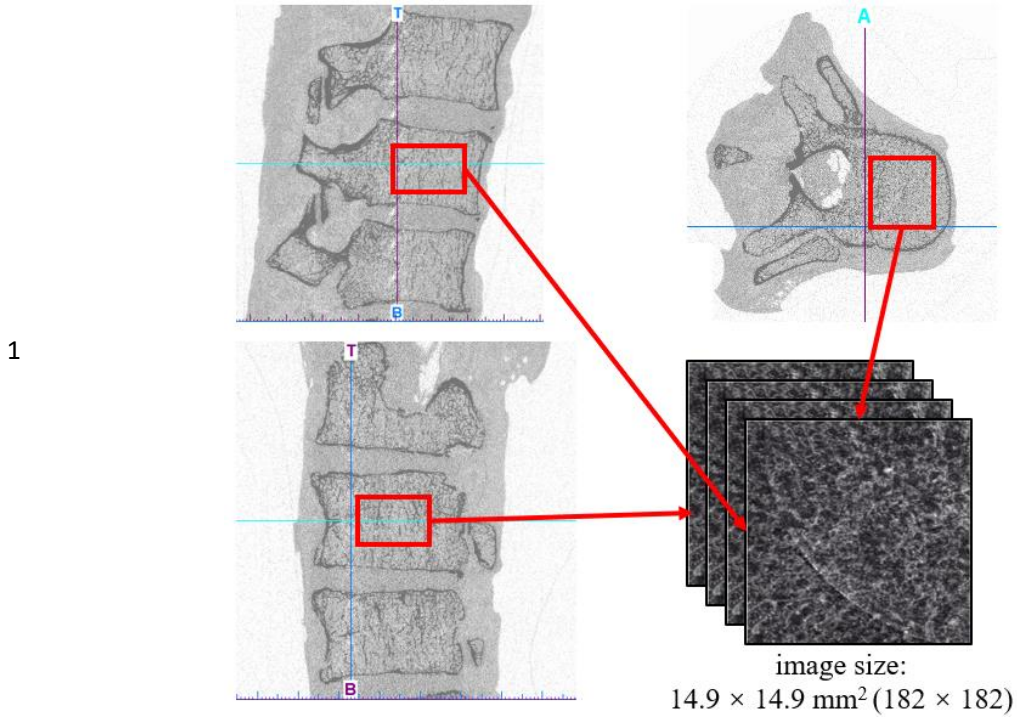
- 1 Eckstein, F., 2002. Mechanical strength of the thoracolumbar spine in the elderly:
2 prediction from in situ dual-energy X-ray absorptiometry, quantitative computed
3 tomography (QCT), upper and lower limb peripheral QCT, and quantitative
4 ultrasound. *Bone*. 31(1), 77-84.
- 5 Lu, Y., Maquer, G., Museyko, O., Puschel, K., Engelke, K., Zysset, P., Morlock, M.,
6 Huber, G., 2014. Finite element analyses of human vertebral bodies embedded in
7 polymethylmethacrylate or loaded via the hyperelastic intervertebral disc
8 models provide equivalent predictions of experimental strength. *J. Biomech.* 47,
9 2512-2516.
- 10 Lu, Y., Krause, M., Bishop, N., Sellenschloh, K., Gluer, C.C., Puschel, K., Amling, M.,
11 Morlock, M.M., Huber, G., 2015. The role of patient-mode high-resolution
12 peripheral quantitative computed tomography indices in the prediction of failure
13 strength of the elderly women's thoracic vertebral body. *Osteoporosis. Int.* 26,
14 237-244.
- 15 Lu, Y., Zhu, Y., Krause, M., Huber, G., 2019. Evaluation of the capability of the
16 simulated dual energy X-ray absorptiometry-based two-dimensional finite
17 element models for predicting vertebral failure loads. *Med. Eng. Phys.* 69, 43-49.
- 18 Metz, C., Duda, G., Checa, S., 2019. Towards multi-dynamic mechano-biological
19 optimization of 3D-printed scaffolds to foster bone regeneration. *Acta Biomater.*
20 101,117-127.
- 21 Omairey, S., Dunning, P.D., Sriramula, S., 2019. Development of an ABAQUS plugin
22 tool for periodic RVE homogenization. *Eng. Comput.* 35(5), 567-577.
- 23 Pistoia, W., Rietbergen, B., Lochmuller, E.M., Lill, C.A., Eckstein, F., Ruegsegger, P.,
24 2002. Estimation of distal radius failure load with micro-finite element analysis
25 models based on three-dimensional peripheral quantitative computed
26 tomography images. *Bone*. 30(6), 842-848.
- 27 Rane, L., Ding, Z., McGregor, A.H., Bull, A.M.J., 2019. Deep learning for
28 musculoskeletal force prediction. *Ann. Biomed. Eng.* 47(3), 778-789.
- 29 Rubio, J., Angelov, P., Pacheco, J., 2011. Uniformly Stable Backpropagation
30 Algorithm to Train a Feedforward Neural Network. *IEEE. T. Neural. Networ.*

1 22(3), 356-366.

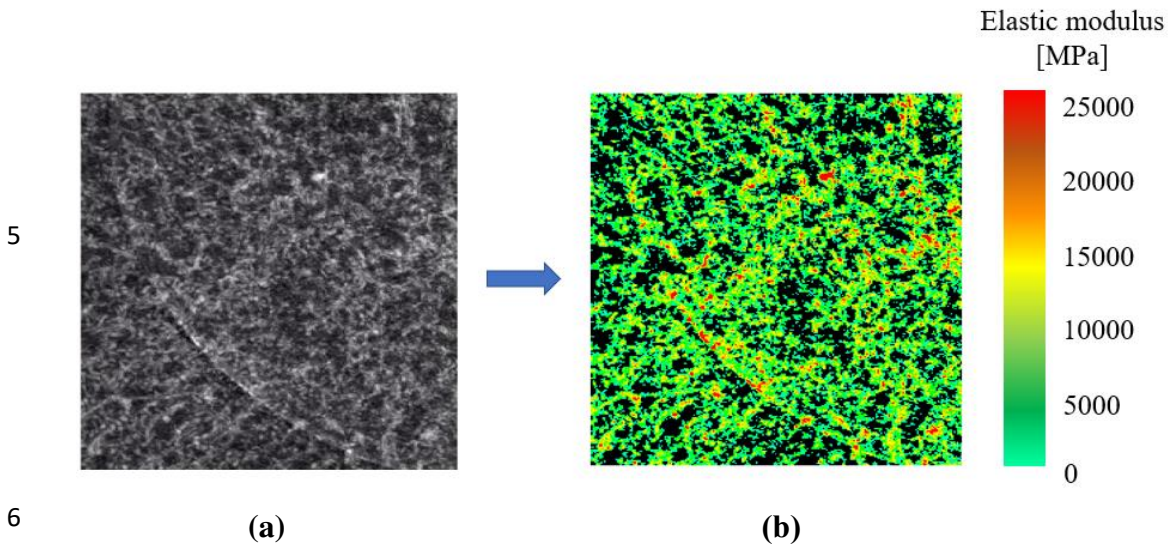
2 Wang, X., Sanyal, A., Cawthon, P.M., Christensen, J., Ensrud, K.E., Cummings, S.R.,
3 Orwoll, E., Black, D.M., Keaveny, T.M., 2012. Prediction of new clinical
4 vertebral fractures in elderly men using finite element analysis of CT scans. *J.*
5 *Bone. Miner. Res.* 27(4), 808-816.

6 Ye, S., Li, B., Li, Q., Zhao, H., Feng, X., 2019. Deep neural network method for
7 predicting the mechanical properties of composites. *Appl. Phys. Lett.* 115,
8 161901.

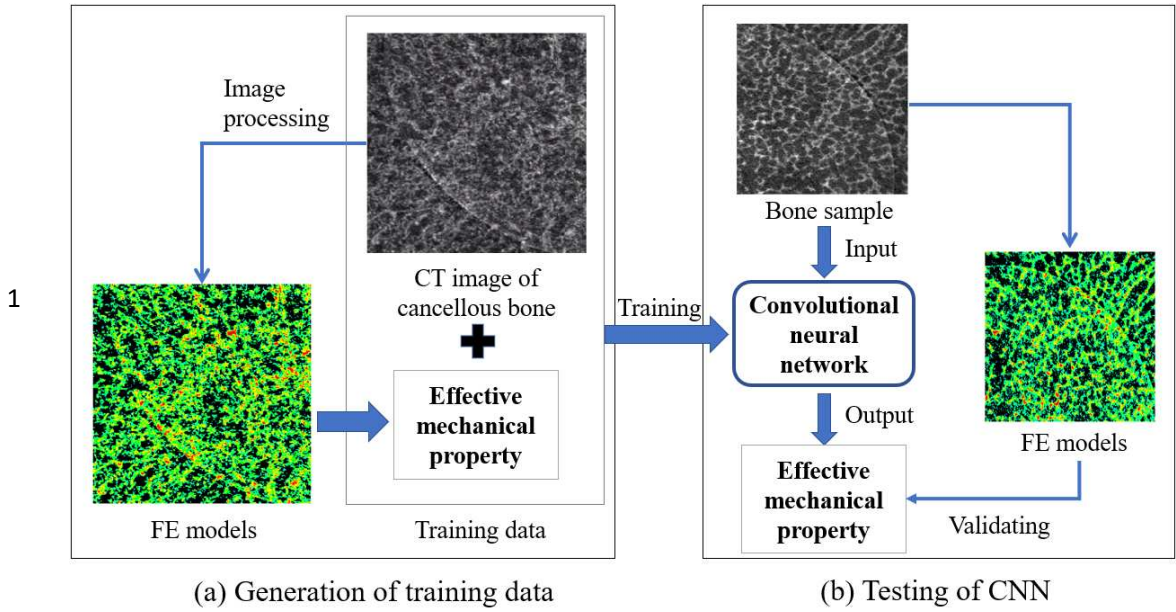
9



2 **Figure 1.** Extraction of the CT data of the human cancellous bone for the construction
 3 of the convolutional neural network model.
 4

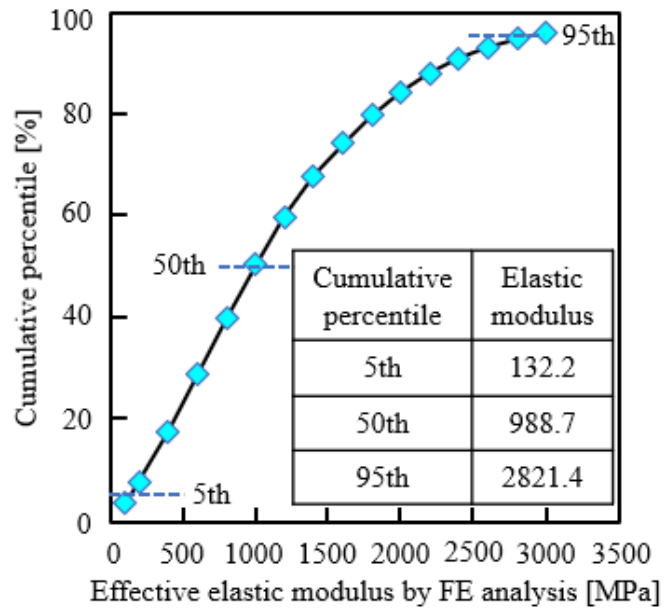


7 **Figure 2.** Establishment of the heterogeneous finite element model for calculating the
 8 effective elastic modulus of bone tissues.
 9
 10



2 **Figure 3.** The workflow for the training and testing of the convolutional neural
 3 network (CNN) model.

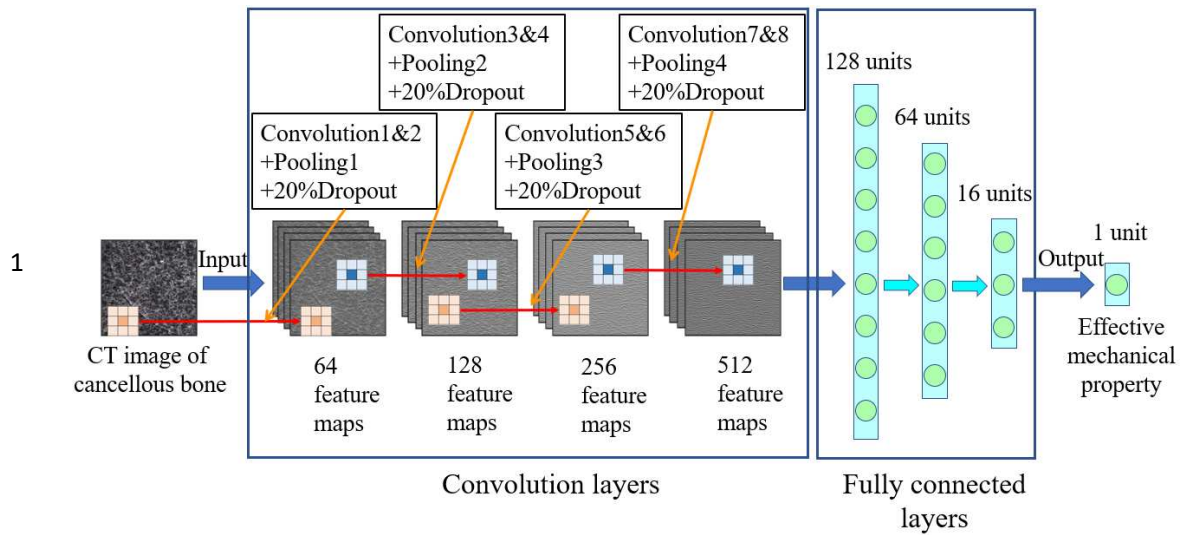
4



5

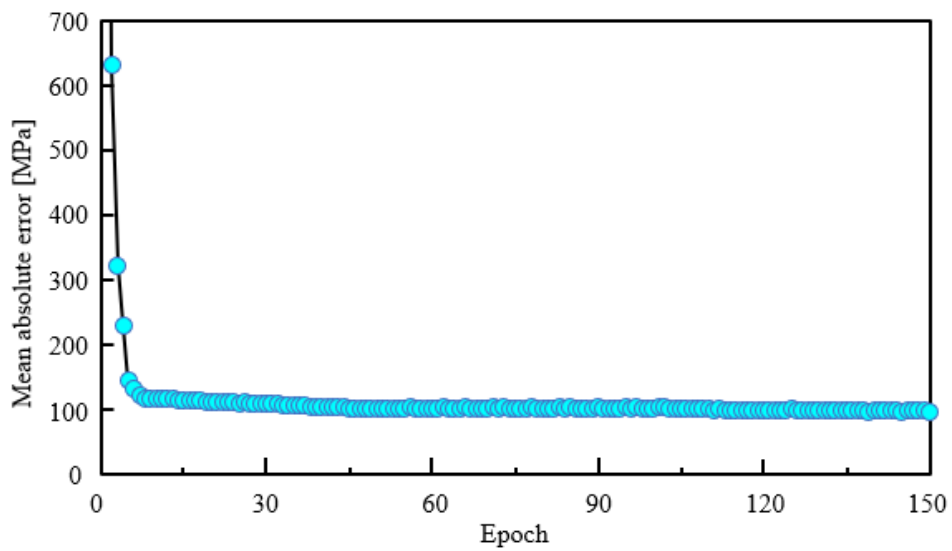
6 **Figure 4.** Distribution of the effective elastic moduli of bone samples used in the
 7 present study (all the bone samples, N = 10636).

8



2 **Figure 5.** The convolutional neural network model constructed in the present study.

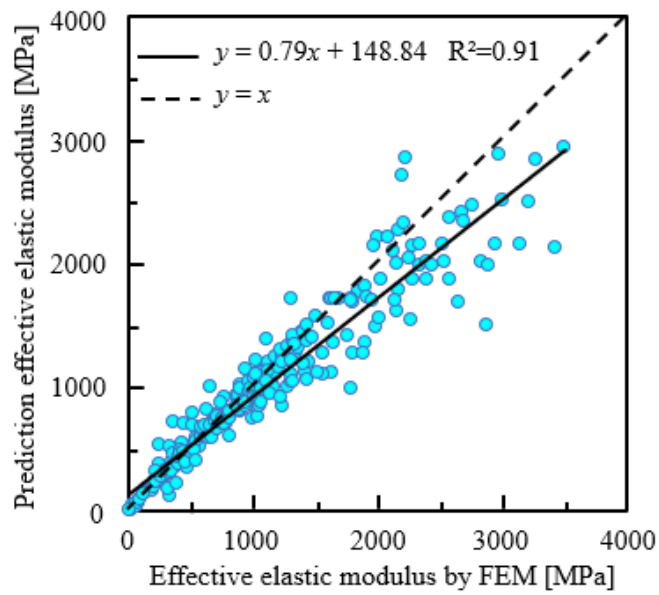
3



4

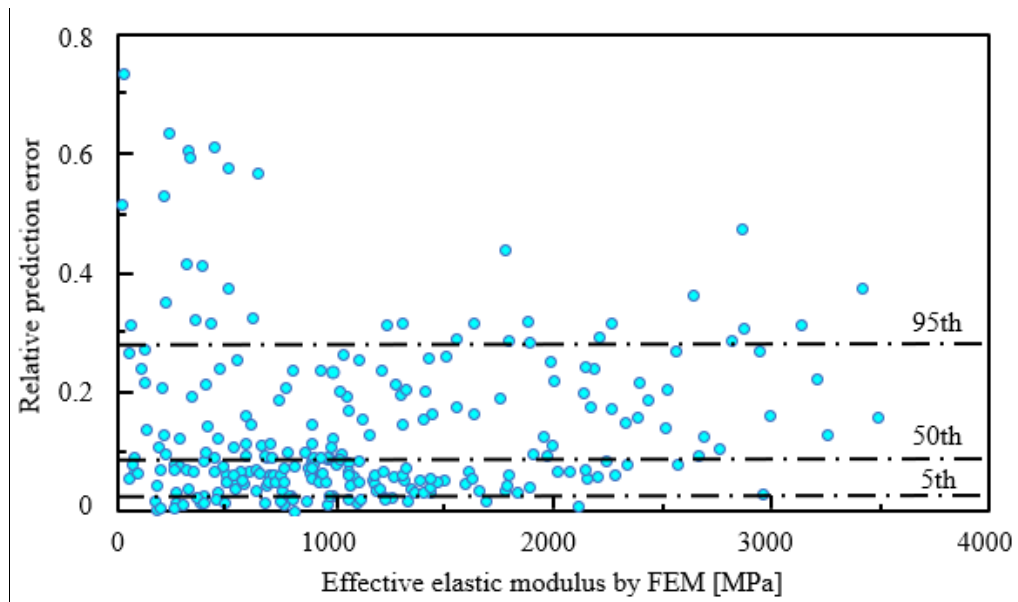
5 **Figure 6.** The relationship between the mean absolute error and the Epoch.

6



1
2
3
4
5

Figure 7. The relationship between the effective elastic moduli predicted from the convolutional neural network (CNN) model and those calculated from the finite element method (FEM)

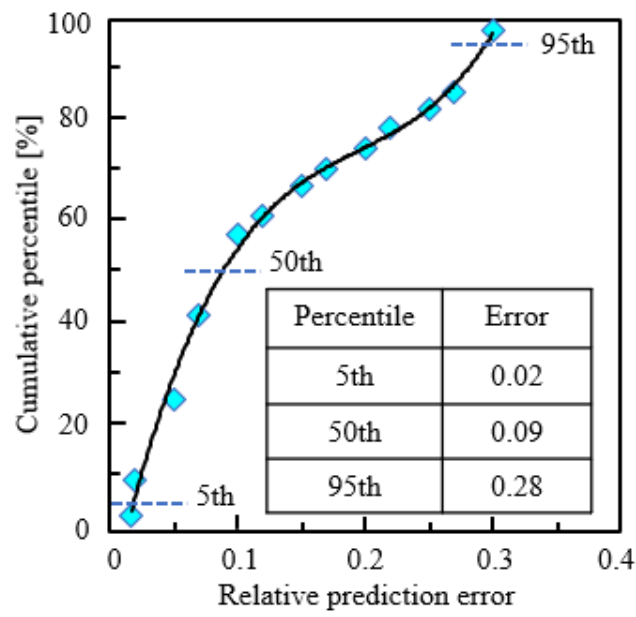


6
7
8
9
10

Figure 8. Distribution of the relative prediction errors of the convolutional neural network model

1

2



3

Figure 9. The relationship between the cumulative percentile and the relative prediction error of the convolutional neural network model

4

5

6